Effects of Fiber Orientation on Ballistic Impact upon Polymer Composite Plate

Kumrungsie[1], Kuntinee Maneeratana[1] and Nuwong Chollacoop[2]

[1] Department of Mechanical Engineering, Chulalongkorn University, Bangkok 10330
Tel. 0-2218-6639, Fax. 0-2252-2889,.E-mail:prayut_kum@hotmail.com, kuntinee.m@chula.ac.th
[2] National Metal and Materials Technology Center (MTEC), Pathumthani 12120
Tel. 0-2564-6500 ext 4700, Fax. 0-2564-6403, E-mail: nuwongc

Abstract

This article concerns with the simulation of ballistic impact on polymer composite with in-plane bidirectional-fiber direction instead of unidirectional as in our previous work [1], which was inspired by Gu & Xu [2]. The models consist of bullet impact on 5-mm-thick polymer composite plates with different side lengths and boundary conditions. The LS-DYNA FEM package is used to simulate the impact result. The bullet is rigid while the composite armor plate is modeled by the type-22 composite damage material with Twaron®/epoxy composite properties. The simulation reveals that the stress waves progress outwards from the point of impact in both fiber directions to the target edges unlike the domination of wave movement along the single fiber direction in the unidirectional plate. The residual bullet velocities from impact on bidirectional plates are lower than those on the unidirectional plates. The fixed edge condition acts as an artificial boundary stiffener when the plate is not sufficiently large such that the reflected stress waves and zero boundary displacement interfere with the perforation mechanisms.

Keywords: Ballistic impact, polymer composite, LS-DYNA

1. Introduction

The National Metal and Materials Technology Center (MTEC) has initiated a project to develop the locally-made, light weight hard armor. The numerical simulation is used to analyze ballistic impacts on armors in order to obtain rough guidelines, particularly parameter adjustments for the prototype configuration.

Even though new composites have been developed for the project [3], their properties have yet to be reliably obtained. Thus, it was decided to proceed to formulate computational simulation which can be compared and verified with a previous literature [2] such that a template model can be obtained for further investigations with newly developed composites.

During the preliminary study, it was found that the ABAQUS finite element package is not best suited for the task due to the anisotropic and dynamic material behaviors of composite armor plates. Thus, an alternative commercial finite element code LS-DYNA [4], which has been popular for dynamic problems, is chosen instead.

Our previous work [1] was well-calibrated with the experimental and numerical results from Gu & Xu [2]. However, the model was based on the unidirectional-fiber composite whereas the real composites under development [3] are made up of bidirectional or woven fibers. Thus, this work aims to extend the previous model to the bidirectional-fiber composite with some variations of plate size and boundary conditions.

2. Material Characterization

The composite is modeled as a transversely isotropic material, employing the LS-DYNA material type 22 (composite damage model), which is based on Chang-Chang criterion [5] with the stress-strain relationship as follows:

$$\varepsilon_1 = \frac{\sigma_1 - \nu_1\sigma_2}{E_1},\ \varepsilon_2 = \frac{\sigma_2 - \nu_2\sigma_1}{E_2},\ \varepsilon_{12} = \frac{\tau_{12}}{2G_{12}} + \frac{\alpha\tau_{12}^3}{2} \quad (1)$$

where ε_1 and ε_2 are respectively normal strains which are respectively parallel and perpendicular to fiber direction; ε_{12} is the in-plane shear strain; σ_1, σ_2 and τ_{12} are stresses which correspond to ε_1, ε_2 and ε_{12}, respectively. The moduli E_1, E_2 and G_{12} are stiffness constants in the same order. The ν_1 and ν_2 are Poisson's ratio in 1 and 2 in-plane directions while α is the nonlinear parameter of shear stress.

These fiber-reinforced composites are approximated to be transversely isotropic. Thus, five independent elastic constants are needed to fully describe their elastic properties. The matrix is considered to be isotropic with three independent elastic material constants. All independent parameters of the composite can be calculated using the microstructure approach. Some parameters, such as G_{23} and ν_{23} that can not be calculated from the microstructure approach due to the physical meaning incompatibility in 3D composites, can be obtained from the assumption of transverse material in the unidirectional lamina. From the elastic constant parameters and critical strength of lamina, the LS-DYNA algorithm predicts damage from matrix cracking followed by fiber tensile failure and composite compressive failure, if any.

Failure of a composite occurs when the combined stresses reach a critical value, which may result from fiber fracture, matrix cracking or compressive failure in

accordance with the following rules.

(a) Fiber fracture ($F_{fiber} \geq 1$): When a fiber is fractured, the mechanical properties E_1, E_2, G_{12}, ν_1 and ν_2 are all set to zero.

$$F_{fiber} = \left(\frac{\sigma_1}{S_1}\right)^2 + \bar{\tau} \tag{2}$$

(b) Matrix cracking ($F_{matrix} \geq 1$): When matrixes fail, E_2, G_{12}, ν_1 and ν_2 are all set to zero.

$$F_{matrix} = \left(\frac{\sigma_2}{S_2}\right)^2 + \bar{\tau} \tag{3}$$

(c) Compressive failure ($F_{comp} \geq 1$): When compressive failures occur, E_2, ν_1 and ν_2 are set to zero.

$$F_{comp} = \left(\frac{\sigma_2}{2S_{12}}\right)^2 + \left[\left(\frac{C_2}{2S_{12}}\right)^2 - 1\right]\frac{\sigma_2}{C_2} + \bar{\tau} \tag{4}$$

A fiber matrix shearing term augments each damage mode such that:

$$\bar{\tau} = \left(\frac{\tau_{12}^2}{2G_{12}} + \frac{3}{4}\alpha\tau_{12}^4\right) \Big/ \left(\frac{S_{12}^2}{2G_{12}} + \frac{3}{4}\alpha S_{12}^4\right) \tag{5}$$

where S_1, S_2, S_{12} and C_2 are longitudinal tensile strength, transverse tensile strength, in-plane shear strength and transverse compressive strength, respectively.

3. Simulation of Uni and Bidirectional-fiber Direction

The 7.95-g conically cylindrical projectile has the diameter and length of 7.87 and 26.8 mm, respectively. The bullet is modeled by 618 4-node tetrahedral elements with LS-DYNA type 20 rigid material.

The 45-mm×100-mm, 5-mm-thick target plate is fixed at the top and bottom and modeled with 25,000 8-node hexahedron elements (Figure 1). The material type 22 composite damage model is chosen to model the bidirectional Twaron®/epoxy plate in which the property is changed from unidirectional, equivalent to the same alignment of fiber layers [1], to bidirectional, in which the fiber layers are aligned perpendicular to one another (Table 1). The directions 1 and 2 represent in-plane direction while 3 represents the out-of-plane orientation.

Table 1 Unidirectional [1] and bidirectional properties

	property	uni	bi
E_1	longitudinal Young's modulus, GPa	20.44	20.44
E_2	transverse Young's modulus, GPa	8.9	20.44
E_3	normal Young's modulus, GPa	8.9	8.9
ν_{21}	Poisson's ratio 21	0.31	0.49
ν_{31}	Poisson's ratio 31	0.31	0.31
ν_{32}	Poisson's ratio 32	0.49	0.31
G_{12}	shear modulus 12, GPa	1.64	6.84
G_{23}	shear modulus 23, GPa	3.03	1.64
G_{31}	shear modulus 31, GPa	1.64	1.64
E_b	bulk modulus of failed material, GPa	20.4	20.4
S_1	longitudinal tensile strength, GPa	1.145	1.145
S_2	transverse tensile strength, GPa	1.13	1.145
C_2	transverse compressive strength, GPa	0.65	0.65
S_{12}	in-plane shear strength, GPa	0.39	0.39
α	nonlinear parameters of shear stress	0	0
ρ	mass density, g/cm^3	1.23	1.23

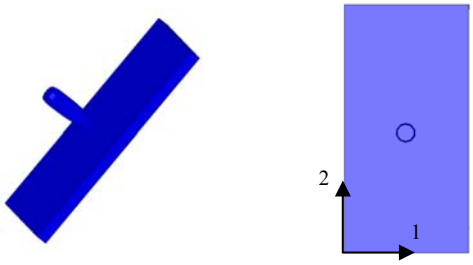

model initial step

Figure 1 The computational model setup

When the bullet hit the target with unidirectional-fiber orientation, the stress is mainly dissipated along the fiber longitudinally to the top and bottom due to the higher stress wave velocity from the higher material strength in that direction (Figure 2) as in [1].

For the bidirectional-fiber plate, the stress contours (Figure 3) shows that the stress wave is initiated from the point of impact in both in-plane directions and expands towards target edges (e.g. t = 15 and 30 μs) because of the bidirectional properties of the composite. Later, the stress wave starts to elongated lengthwise (e.g. t = 60 and 75 μs) due to the fixed boundary condition, followed by the wave reflection at the clamp (e.g. t = 90 μs).

The bullet horizontal velocity decreases with time due to the resistance of the armor plate during impact (Figure 4). After full perforation, the bullet velocity is leveled off at the residual velocity. As expected, the bidirectional target yields a lower residual velocity by absorbing more energy. The bidirectional plate also shows less deformation around the impact locality.

When the side views of the impact are visually inspected (Figure 2 and Figure 3), the side edges, which are not constraint, are noticeably deformed and curved from the bullet impacts for both uni and bidirectional-fiber plates. In addition, the energy history of the plate (Figure 5) shows sporadically changes in internal and kinetic energy components while the sum of both energy components remains relatively steady after the bullet punches through the plate. This characteristic may be due to the stress wave propagation and the boundary conditions which is further investigated next.

4. Effects of Fixed Boundary Condition

The 45-mm×100-mm, 5-mm-thick target plate, as in the previous section, is fixed at all edges in the simulations with the same material properties.

Figure 6 and Figure 7 show the Mises stress contours during the perforation of the unidirectional and bidirectional-fiber plates, respectively. While the stress contour characteristics, which are found in the previous cases, are still observed, the side edges are subjected to high stress due to the fixed boundary condition.

With magnified visual inspection, less gross deformation of the plates are observed in both uni and bidirectional-fiber plates when all edges are constrained with fixed boundary instead of leaving the side edges free to bend, reminiscing a stiffening effects on the plates.

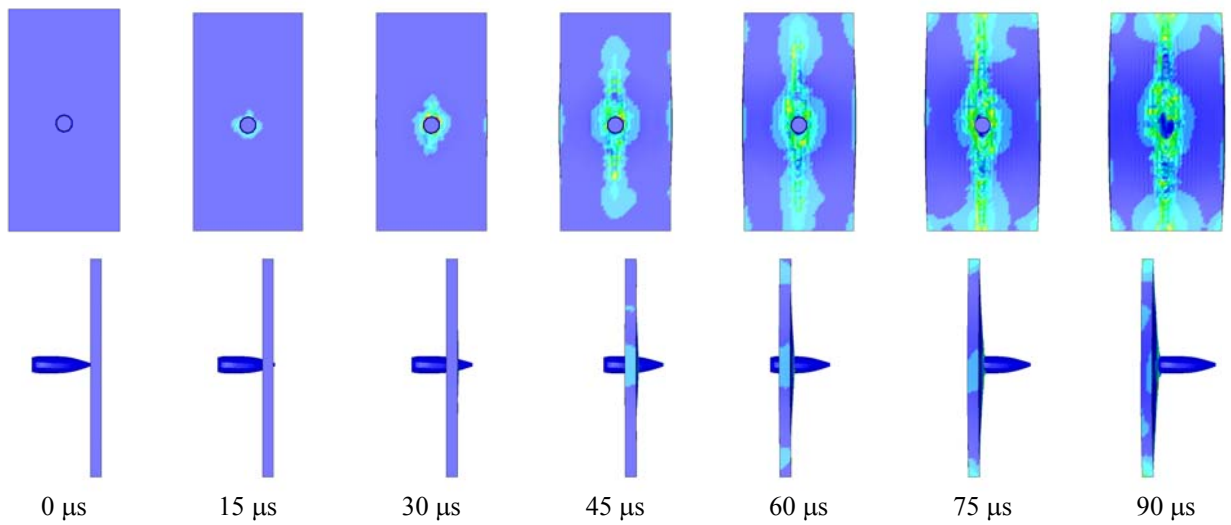

Figure 2 Mises stress contours and perforation at various time instants *t* from 390 m/s bullet impact on a unidirectional-fiber plate with fixed top and bottom edges, resulting in 359 m/s residual velocity. The color blue represents no stress while red is for 1.0 GPa.

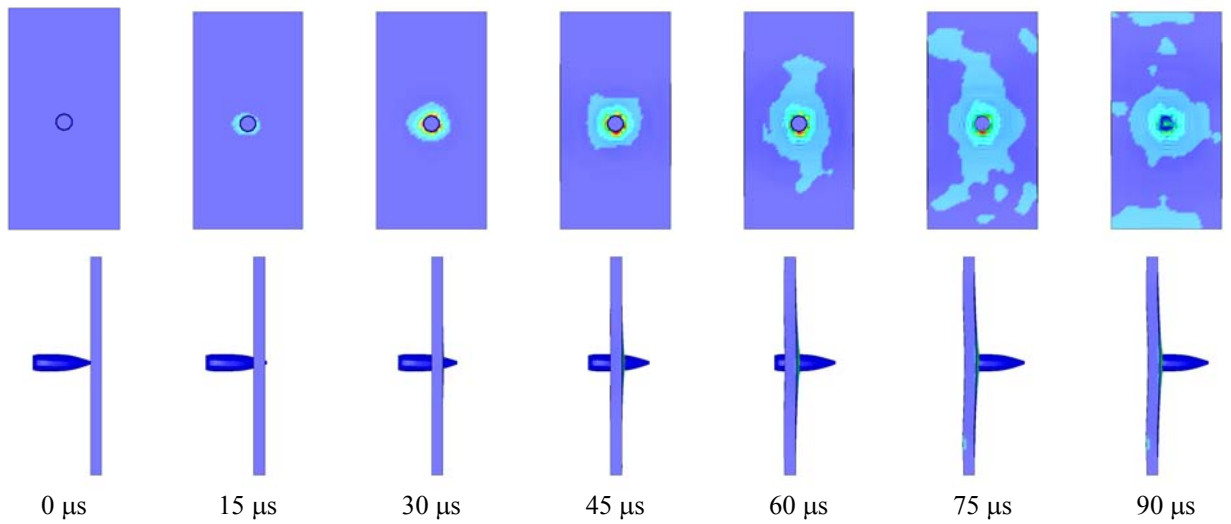

Figure 3 Mises stress contours and perforation at various time instants *t* from 390 m/s bullet impact on a bidirectional-fiber plate with fixed top and bottom edges, resulting in 344 m/s residual velocity. The color blue represents no stress while red is for 1.0 GPa.

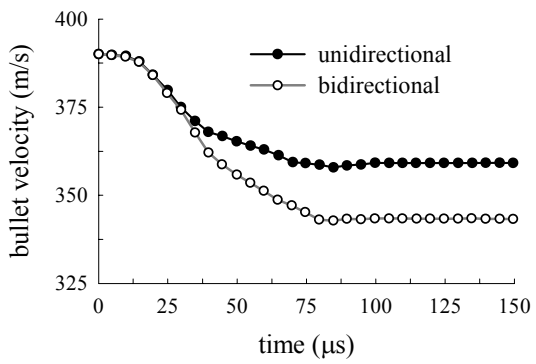

Figure 4 Bullet velocities during the perforation from 390 m/s bullet impact on the plates with fixed top and bottom edges

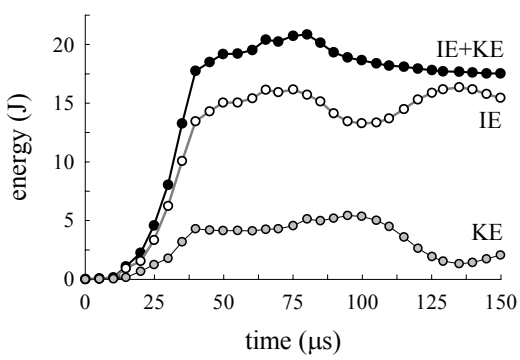

Figure 5 Internal energy (IE) and kinetics energy (KE) of the bidirectional-fiber plates with fixed top and bottom edges during the perforation from 390 m/s bullet impact

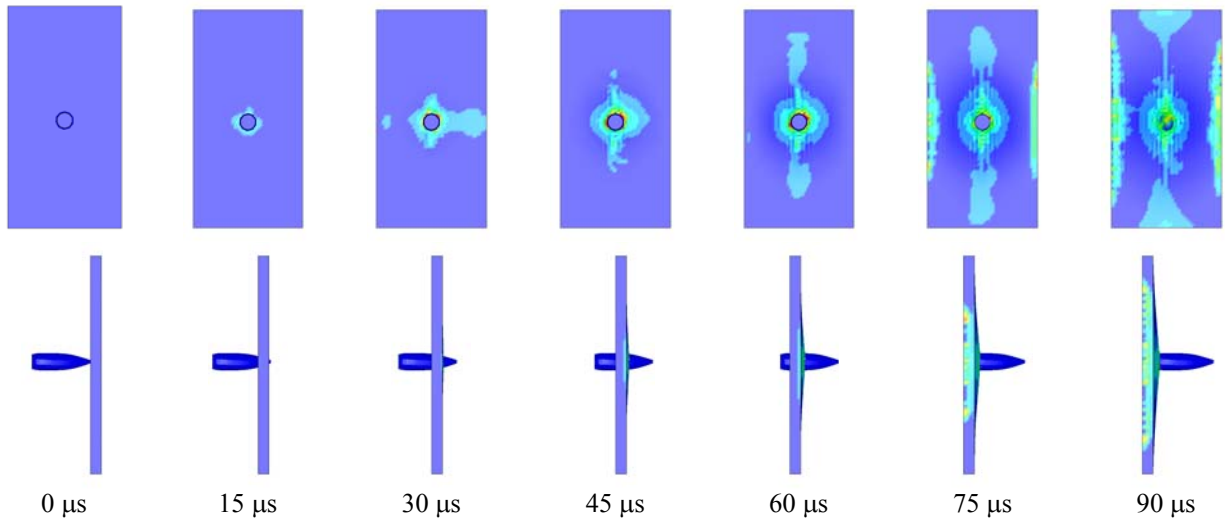

Figure 6 Mises stress contours and perforation at various time instants *t* from 390 m/s bullet impact on a unidirectional-fiber plate with fixed edges, resulting in 349 m/s residual velocity. The color blue represents no stress while red is for 1.0 GPa.

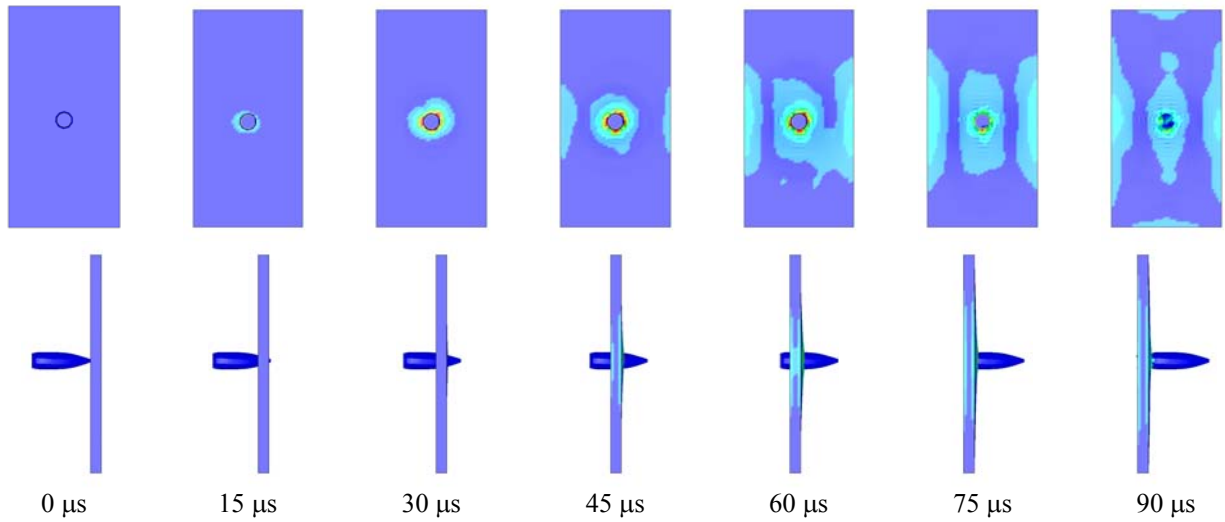

Figure 7 Mises stress contours and perforation at various time instants *t* from 390 m/s bullet impact on a bidirectional-fiber plate with fixed edges, resulting in 339 m/s residual velocity. The color blue represents no stress while red is for 1.0 GPa.

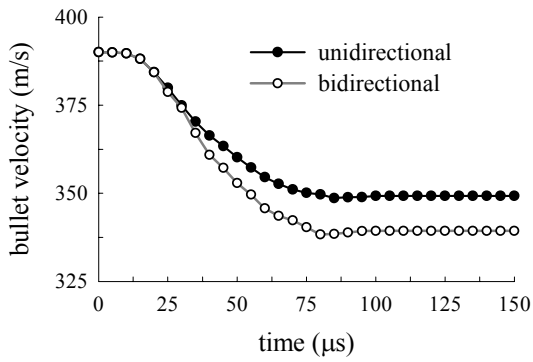

Figure 8 Bullet velocities during the perforation from 390 m/s bullet impact on the plates with fixed edges

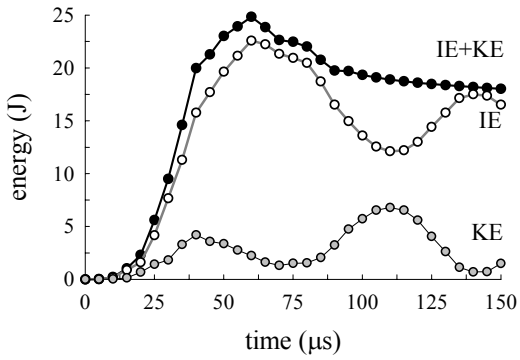

Figure 9 Internal energy (IE) and kinetics energy (KE) of the bidirectional-fiber plates with fixed edges during the perforation from 390 m/s bullet impact

When the residual velocities are compared (Figure 8), the bidirectional-fiber plate still better resists the bullet impact. However, both residual velocities when all edges are fixed are lower than the cases in which only the top and bottom edges are fixed (Figure 4), indicating better resistance from the boundary condition.

Moreover, the energy history of the plate (Figure 9) shows even more variation in internal and kinetic energy components. This further strengthens the possibility that the observed characteristics are geometrical and boundary dependent, which leads to the simulation of the different plate geometry in the next section.

5. Simulation of Bidirectional Square Plate

In order to confirm the size and boundary condition effects on the simulation with bidirectional-fiber material, these effects should be reduced or eliminated by increasing the plate size such that they can not interfere with the perforation mechanism during the bullet impact.

Thus, 5-mm-thick plates of increasing sizes – 100-mm×100-mm, 200-mm×200-mm and 300-mm×300-mm – are used in the simulation of bullet impact at 390 m/s (Figure 10). The plates are discretized into 50,000, 222,585 and 450,000 8-node hexahedron elements, respectively.

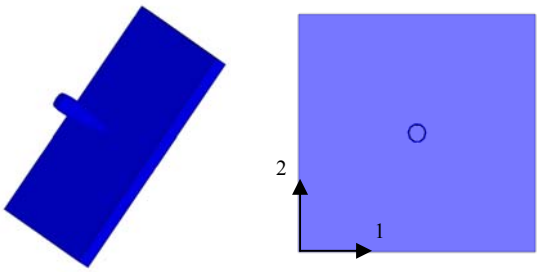

model initial step

Figure 10 The square model setup

Table 2 shows the Mises stress contours and the side-view perforation of the bidirectional-fiber plates of different sizes. The smallest plate, 100-mm×100-mm, clearly shows the wave reflections at the edges, indicating that it is not large enough for the purpose. Meanwhile, the two bigger plates experience truly significant stress at the centers.

When the residual velocities (Figure 11) are considered, it is found that the residual velocity from the 100-mm×100-mm fixed plate is higher than the 45-mm×100-mm fixed plate (Figure 8), further indicating that the better impact resistance of the smaller plate may be due to the boundary constraint. As the plate gets bigger, the residual velocity decreases slightly at a decreasing rate, showing insignificant differences between the 200-mm×200-mm and 300-mm×300-mm plates.

These results may seem contradicting, but when the energy components in the plates are compared, it is clear that the boundary interference is still present in the 100-mm×100-mm plate (Figure 12a) while these sporadically changes in internal and kinetic energy components are not presented in the larger plates (Figure 12b and Figure 12c). In addition, small change in internal energy can be clearly observed when the bullet is about to leave the plate. It is also clear that the plate still pulsate long after the bullet punches through, as shown by a longer time axis in Figure 12a. Therefore, larger plates are needed when only the initial impact resistance of the material is studied.

This argument also implies that the plate size and boundary condition, i.e. armor plate installation method, must be carefully studied to truly ensure the required performances.

6. Conclusion

Preliminary results show the capability of extending the well-calibrated computational model from the unidirectional-fiber composite plate to the bidirectional one to better emulate the composite armor prototype under development. The computational model shows that bidirectional plate absorbs more energy, resulting in a lower residual velocity of the penetrated bullet. It is also noted that the plate size and boundary conditions may influence the armor plate integrity.

This investigation serves as a guideline for future optimization of the armor plate prototype. The current framework thus planned is to experimentally measure the values of the composite properties and use them in the simulation for verification and possibly prediction of the plate behavior upon ballistic impact as well as further numerical investigation with parametric studies of the plate properties.

Acknowledgements

This research is financially supported by MTEC, contract no. MT-B-48-CER-07-188-I.

References

[1] Kumrungsie, P., Maneeratana, K., and Chollacoop, N., 2007. Simulation of Ballistic Impact on Polymer Composite Armor. 2007 NSTDA Annual Conference (NAC 2007), Thailand Science Park, Pathumthani, March 28-30.

[2] Gu, B., and Xu, J., 2004. Finite Element Calculation of 4-step 3-dimensional Braided Composite under Ballistic Perforation. Composites Part B: Engineering. Vol. 35, No. 4, pp. 291-297.

[3] Amonsukchai, T., and Rimdusit, S., 2004. Development of Polyethylene Fiber, Composites from Benzoxazine-Based Alloys and Polyethylene or Kevlar Fiber and Polymer Composites/Metal or Ceramic for Armory, MTEC report.

[4] Livermore Software Technology Corporation, 2005. LS-DYNA Theoretical Manual. Version 970.

[5] Chang, F. K., and Chang, K. Y., 1987. A Progressive Damage Model for Laminated Composite Containing Stress Concentration. Journal of Composite, Vol. 21, No. 9, pp. 834-855.

Table 2 Mises stress contours and perforation at various time instants *t* and from bullet impact on a bidirectional-fiber square plate with fixed edges at 390 m/s. The color blue represents no stress while and red is for 1.0 GPa.

time	100-mm×100-mm plate	200-mm×200-mm plate	300-mm×300-mm plate
0 μ	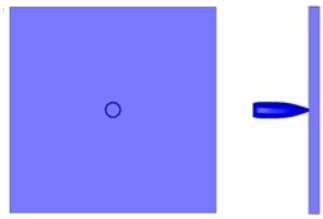		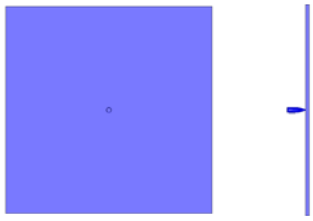
15 μs	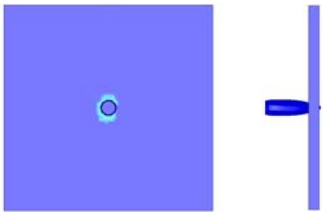	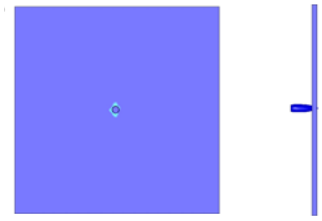	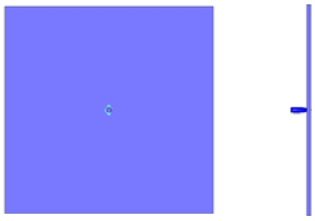
30 μs	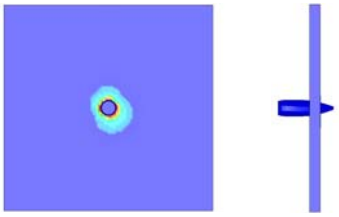	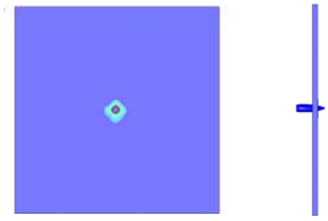	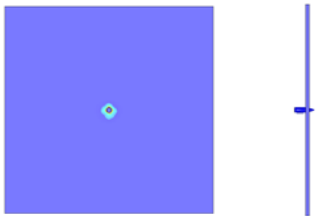
45 μs	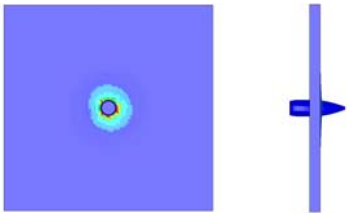	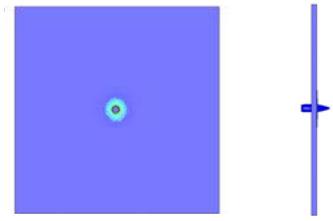	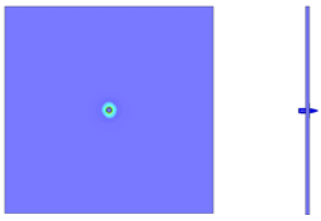
60 μs	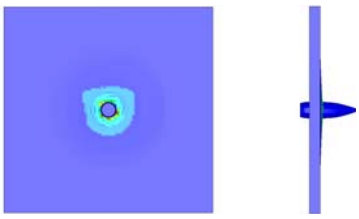	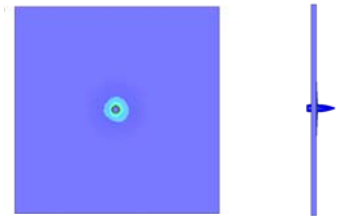	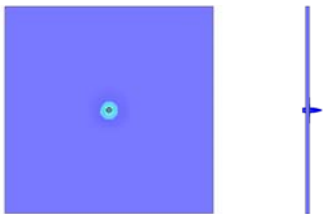
75 μs	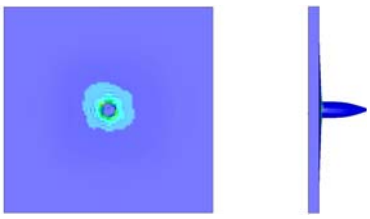	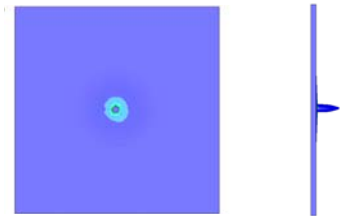	
90 μs	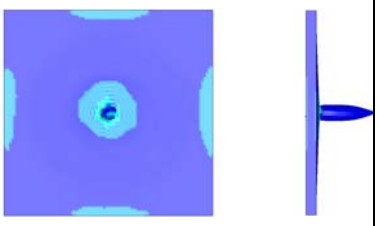		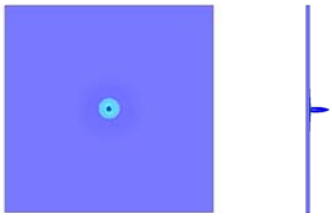
v_r	349 m/s	347 m/s	347 m/s

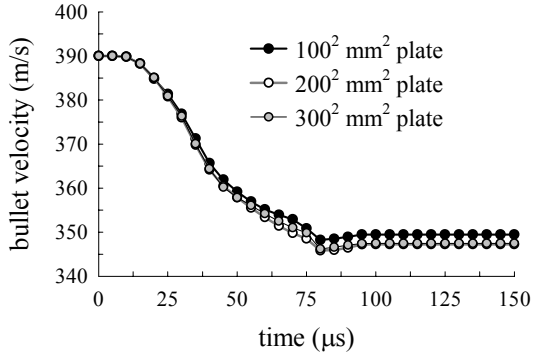

Figure 11 Bullet velocities during the perforation of the square plates with 390 m/s bullet impact

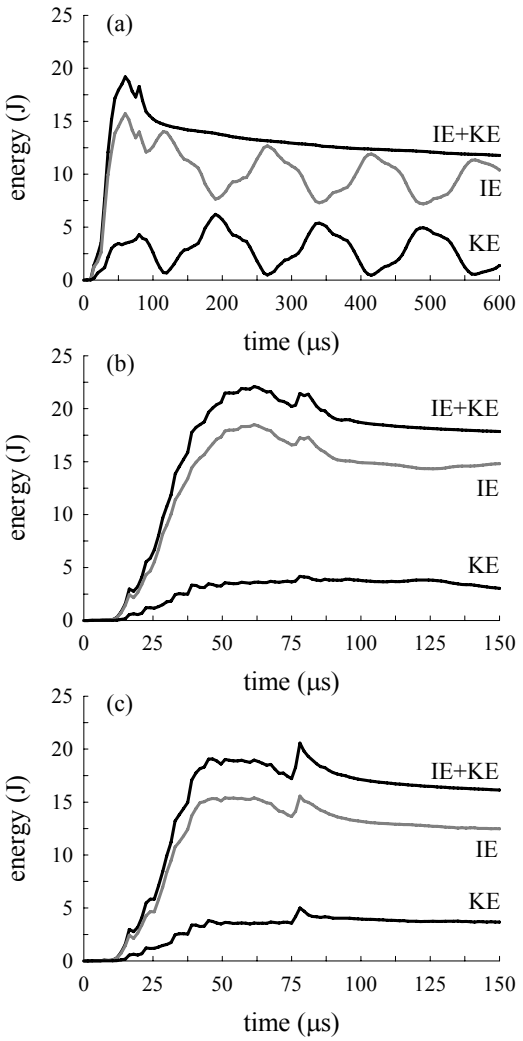

Figure 12 Internal energy (IE) and kinetics energy (KE) of the target plate during the perforation of the (a) 100-mm×100-mm, (b) 200-mm×200-mm and (c) 300-mm×300-mm plates with bullet impact at 390 m/s.